CHAPTER 1

Chemical evolution of autotaxin inhibitors: *An introduction*

Harald M.H.G. Albers and Huib Ovaa, *Accepted for publication in Chemical Reviews.*

Abstract. Autotaxin (ATX) is a potential drug target implicated in various diseases, including cancer. ATX was originally isolated as a tumor cell motility factor from melanoma cells in 1992. It then took a decade to find that ATX has lysophospholipase D activity and is responsible for the production of the bioactive lipid lysophosphatidic acid (LPA). The link between ATX-LPA axis and disease has triggered the development of ATX inhibitors. This chapter focuses on the development of ATX inhibitors described in academic and patent literature covering both lipid-based and small molecule inhibitors, including the ATX inhibitors described in the following chapters of this thesis to place them in context of the current literature.

1.1 Introduction

In 1992, autotaxin (ATX or ENPP2) was isolated as an autocrine motility factor from melanoma cells.[1] The ~120 kDa glycoprotein ATX belongs to a small family named ecto-nucleotide pyrophosphatase and phosphodiesterase (ENPP) which consists of 7 family members.[2] ATX is the only ENPP family member with lysophospholipase D (lysoPLD) activity and is responsible for the hydrolysis of lysophosphatidylcholine (LPC) to produce the bioactive lipid lysophosphatidic acid (LPA) (Scheme 1).[3,4] LPA acts on specific G protein-coupled receptors and thereby stimulates the migration, proliferation and survival of many cell types.[5,6] ATX is produced in various tissues and is the major LPA-producing enzyme in the circulation. After biosynthesis by ATX, LPA is subject to degradation by membrane-bound lipid phosphate phosphatases (LPPs).[7,8]

ATX is essential for vascular development[9,10] and is found overexpressed in various human cancers.[11] Forced overexpression of ATX or individual LPA receptors promotes tumor progression in mouse models,[12-15] while LPA receptor deficiency protects from colon carcinogenesis.[16] In addition, to its role in cancer, ATX-LPA signaling has been implicated in lymphocyte homing and (chronic) inflammation,[17] fibrotic diseases,[18,19] thrombosis[20] and cholestatic pruritus.[21] Given its role in human disease, the ATX-LPA axis is an interesting target for therapy that deserves significant attention. The fact that ATX is an extracellular enzyme makes it even more attractive as a drug target.

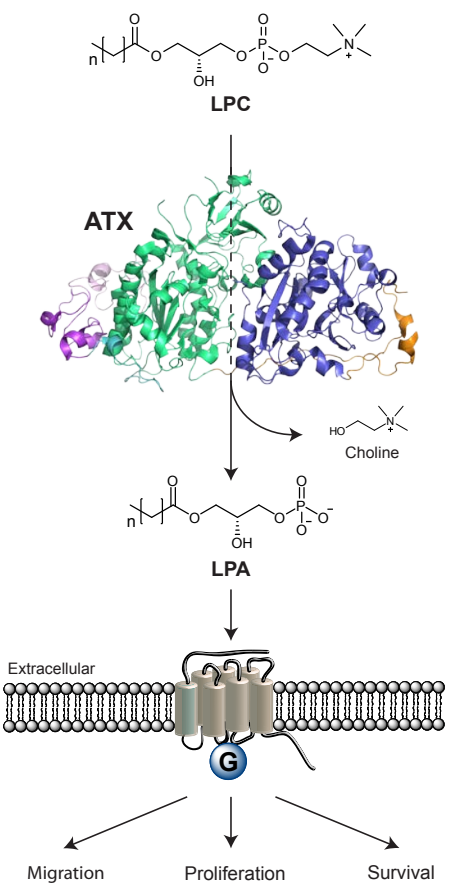

Scheme 1: ATX is responsible for hydrolyzing LPC into LPA in an extracellular environment. This reaction is catalyzed by a threonine residue and two zinc ions present in the ATX active site. LPA activates specific G protein-coupled receptors stimulating migration, proliferation and survival of cells. ATX is displayed as a cartoon representation of the crystal structure (PD ID 2XR9) with the SMB domains in purple, the PDE domain in green and the nuclease-like domain in blue.

1.2 ATX protein

Alternative splicing of the ATX gene (enpp2) results in three distinct isoforms (α, β and γ) which are differentially expressed.[22,23] ATX β (863 aa) is the best studied isoform and is identical to plasma lysoPLD. ATX β is mainly expressed in peripheral tissues, whereas lower

expression levels are observed in the central nervous system. In contrast, the ATX γ (889 aa) isoform is predominately expressed in the central nervous system. ATX α (915 aa), the original melanoma-derived isoform, exhibits the lowest expression levels in both the central nervous system and peripheral tissues. The ATX α isoform contains a non-specific protease cleavage site which is not present in the other isoforms.[22] All the three ATX isoforms exhibit similar catalytic activities *in vitro*.[22]

ATX is produced initially as a pre-pro-enzyme that has an N-terminal signal peptide required for secretion.[24] This signal peptide is removed by a signal peptidase and ATX is subsequently cleaved by proprotein convertases (PCs) like furin.[24] The removal of an N-terminal octapeptide in ATX by PCs is associated with an enhancement of ATX activity.[24] The proteolytically processed ATX is secreted and it consists of several domains. Starting from its N-terminus ATX has two somatomedin B (SMB)-like domains, a central catalytic phosphodiesterase (PDE) domain and an inactive nuclease-like domain as displayed in Scheme 1. The hydrolytic activity of ATX predominately originates from a threonine residue and two zinc ions in the ATX active site located in the PDE domain.[25] Extending from the ATX active site there is a hydrophobic pocket where the alkyl chain of its lipid substrates binds.[26]

1.3 Natural substrates of ATX

Next to LPC hydrolysis, ATX is also capable of hydrolyzing sphingosylphosphorylcholine (SPC, Figure 1) into sphingosine 1-phosphate (S1P).[27] S1P has signaling properties comparable to those of LPA while acting on S1P receptors.[28-30] It is however, doubtful how relevant the contribution of ATX is to S1P production *in vivo*. S1P is thought to originate mainly from the phosphorylation of sphingosine by sphingosine kinases, rather than through SPC hydrolysis by ATX.[31]

Next to recognizing the lipids LPC and SPC as substrates, ATX can also hydrolyze nucleotides, like its family members ENPP1 and ENPP3. *In vitro* established nucleotide and nucleotide-derived substrates of ATX consist of adenosine-5'-triphosphate (ATP), diadenosine polyphosphates (Ap_nA), uridine diphosphate glucose

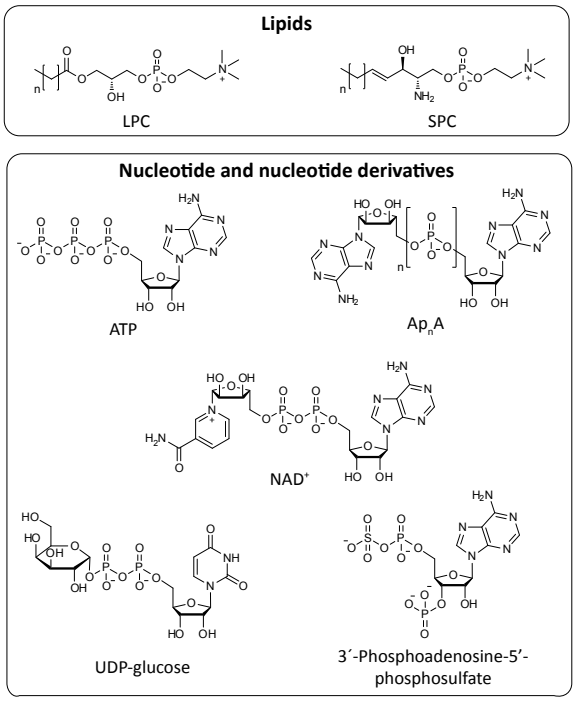

Figure 1: Identified natural substrates of ATX.

(UDP-glucose), nicotinamide adenine dinucleotide (NAD^+) and 3'-phosphoadenosine-5'-phosphosulfate (Figure 1).[2] The physiological relevance of ATX-mediated hydrolysis of these nucleotide substrates is still unclear.

1.4 Assays to study ATX activity

In the search for inhibitors, appropriate *in vitro* assays are required to monitor the activity of the enzyme of interest. Over the last ten years various assays have been developed and used to study the activity of ATX. ATX assays can roughly be divided in two classes depending on the kind of ATX substrate used for the activity measurement. The first class uses the physiological ATX substrate LPC and the second class uses unnatural ATX substrates.

1.4.1 LPC-based assays

As depicted in Table 1, ATX hydrolyzes LPC into LPA and choline. Both products can be used to measure ATX activity. When a ^{14}C label is introduced in the lipid tail of LPC, ATX activity can be measured by radiometry.[32,33] When radiolabeled LPC is hydrolyzed by ATX the produced LPA contains this radiolabel. After lipid extraction of the ATX-LPC incubation mixture and separation of LPC and LPA using thin layer chromatography (TLC),[4] activity of ATX can be quantified from the ^{14}C-LPA product. Although this classical method is robust and very sensitive it is not very suitable for high-throughput screening (HTS).

Another way to measure the formation of LPA is by using liquid chromatography–tandem mass spectrometry (LC-MS/MS).[34,35] From an ATX incubation mixture, LPC and LPA are separated by LC and detected by tandem MS. This method is very sensitive and suitable to detect naturally occurring LPA in biological fluids (i.e. plasma).[34-36]

ATX activity can also be measured by the detection of choline.[4,37] When choline is released from the ATX-mediated LPC hydrolysis it can be converted by choline oxidase into betaine (trimethylglycine) and hydrogen peroxide. Subsequently, hydrogen peroxide is used by horseradish peroxidase (HRP) to convert a coloring substrate into its oxidized chromophoric state. Different HRP coloring substrates can be used like 2,2'-azino-bis(3-ethylbenzothiazoline-6-sulphonic acid) (ABTS), homo-vanillic acid (HVA) or Amplex red. ABTS can be detected using absorbance while HVA and Amplex red are detected by fluorescence.[36,38,39] The throughput of this assay is high and suitable for HTS screening.

A danger of the latter assay is that small molecules that don't inhibit ATX may interfere with the readout by inhibiting the enzymes (HRP or choline oxidase) used in the coloring reaction, which will result in false positives. Another possibility what could result in false positives is that reactive compounds tested in this assay can react with the coloring agent or hydrogen peroxide that is generated during that coloring reaction. Incubating the molecules that are active in this assay with only choline and subsequently adding the coloring reagents should reveal if identified actives are interfering with the assay readout.[38]

Table 1: Substrates for ATX-activity assays.

ATX substrate	Detectable product	References
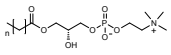 LPC[a]	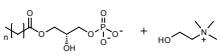	[32] [33] [34] [35] [37]
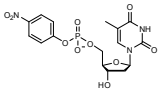 pNP-TMP	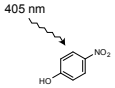	[3] [25]
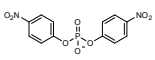 Bis-pNPP	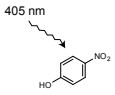	[33] [38]
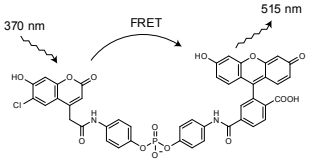 CPF4	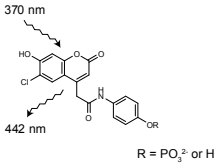 R = PO_3^{2-} or H	[33] [40]
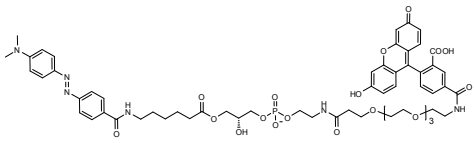 FS3	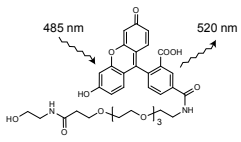	[41]
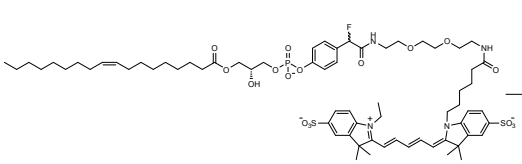 ATX-ABP	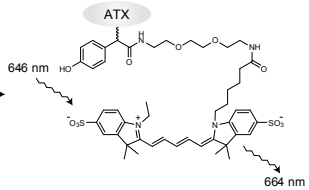	[42]

[a] LPA can be detected by radiometry or mass spectrometry. Choline can be detected in a two-step enzymatic colorimetric reaction.

1.4.2 Unnatural ATX substrate-based assays

As a member of the ecto-nucleotide pyrophosphatase and phosphodiesterase (ENPP) family, ATX also hydrolyzes nucleotides. Therefore, the nucleotide thymidine 5'-monophosphate para-nitrophenyl ester (pNP-TMP) can be used as an ATX substrate (Table 1).[3,25] Upon hydrolysis of pNP-TMP by ATX, 4-nitrophenol is released which has an absorbance at 405 nm and is detectable by colorimetry. The same product is formed when bis-para-nitrophenyl phosphate (bis-pNPP) is hydrolyzed by ATX (Table 1).[33,38] Bis-pNPP is a cheap ATX substrate that provides a direct readout.

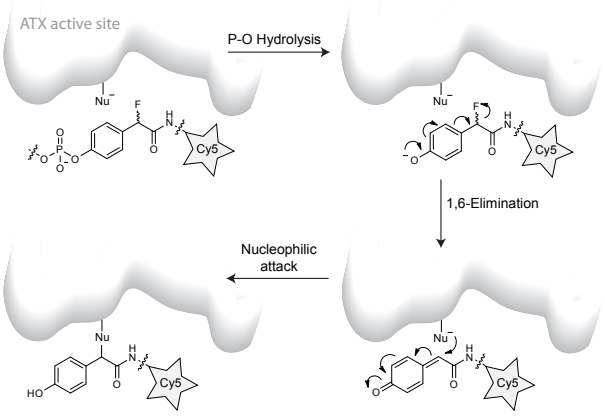

Scheme 2: Labeling mechanism of ATX with ATX-ABP. Only one of the potential labeled products resulting from the labeling is shown.

Another artificial ATX-substrate is CPF4, which has a similar core structure as bis-pNPP. In CPF4 the two nitro groups of bis-pNPP are replaced by coumarin and fluorescein (Table 1).[33,40] When the coumarin donor group in CPF4 is excited Förster fluorescence resonance energy transfer (FRET) between coumarin and the fluorescein acceptor occurs. After hydrolysis the FRET pair is separated and FRET is lost, providing a very sensitive assay reagent. Although this reagent was originally developed for phosphodiesterase I[40] it provides a very sensitive ATX activity sensor as well.[33]

FS3 is another synthetic ATX substrate, which is based on LPC (Table 1).[41] In this substrate a dabcyl moiety, a quencher of fluorescein, is connected *via* a lipid backbone to fluorescein. The fluorescein moiety in FS3 is quenched by the dabcyl moiety and becomes fluorescent when FS3 is hydrolyzed by ATX. A common advantage of the above mentioned assays is that they provide a realtime readout allowing direct kinetic studies of ATX activity.

In addition, a first generation ATX activity-based probe (ATX-ABP) has been reported (Table 1).[42] This probe makes use of the activity of ATX to label ATX covalently. Upon the hydrolysis of the phosphodiester bond in ATX-ABP, the released intermediate undergoes an 1,6-elimination of a fluoride atom (Scheme 2). This generates a reactive quinone methide species that traps nearby nucleophiles in the ATX active site resulting in covalent labeling of ATX with a fluorescent Cy5 dye in an activity-dependent manner. This ATX-ABP is able to label all the three known ATX isoforms.[42] In addition, ATX-ABP can label ATX in human plasma, however, an additional affinity-purifying step with an anti-ATX monoclonal antibody is required to make Cy5 labeled ATX detectable. Further development of this type of probes could turn them into diagnostic reagents to monitor ATX activity in complex samples such as body fluids.

1.5 Inhibitory effect of metal chelators on ATX activity

L-histidine has been reported as the first *in vitro* 'ATX inhibitor' with millimolar IC_{50} values for ATX using LPC or pNP-TMP as assay substrate.[43] It acts by scavenging metal ions in solution, such as zinc, which are essential for ATX activity. In addition, other metal chelating agents such as ethylenediaminetetraacetic acid (EDTA) and 1,10-phenanthroline also have an inhibitory effect on ATX activity.[43]

1.6 Natural lipids and lipid-based inhibitors of ATX

A distinct class of ATX inhibitors are based on lipids. The discovery of product inhibition of ATX by its lipid products LPA and S1P[33] triggered the development of lipid-based ATX inhibitors (Table 2). One class of lipid-based inhibitors includes thiophosphates.[44-46] An example of this class is thiophosphate **3** (IC_{50} = 0.6 µM, bis-pNPP) depicted in Table 2. The reported thiophosphates also act as agonists or antagonists for LPA_{1-3} receptors.[44-46] This is a general danger of lipid-based ATX inhibitors, that they may act on downstream LPA/S1P receptors due to their structural similarity with LPA and S1P.

There is also a class of ATX inhibitors based on cyclic phosphatidic acid (cPA) which is a naturally occurring analog of LPA where the *sn*-2 hydroxy group forms a 5-membered ring with the *sn*-3 phosphate.[47,48] cPA analog **4** (Table 2, IC_{50} = 0.14 µM, bis-pNPP) has no significant agonist activity at LPA receptors. Recently, a sulfur analog of cPA, 3-*O*-thia-cPA (**5**) has been reported as ATX inhibitor (Table 2).[49]

Another class of lipid-based ATX inhibitors is based on α-bromomethylene phosphonates like BrP-LPA (**6**, Table 2).[50,51] In addition, phosphonate **6** acts as a pan LPA_{1-4} receptor antagonist. α-Bromobenzyl phosphonates are well known protein tyrosine phosphatase inhibitors that target the active site covalently.[52] Whether phosphonate **6** inhibits ATX in a covalent manner is unknown. An inhibitor that is expected to bind ATX covalently is flouromethylphenyl phosphate **7** (Table 2).[53] The binding mechanism of **7** with ATX is postulated to be the same as for the ATX-ABP as depicted in Scheme 2.

Interestingly, phosphorylated FTY720 (FTY720-P, **8**, Table 2) inhibits ATX with a K_i of 0.2 µM using pNP-TMP as an ATX assay substrate.[54,55] FTY720-P is a synthetic analog of S1P and acts as an $S1P_1$ receptor antagonist (EC_{50} = 5 nM)[55] that activates this receptor, causing its internalization and subsequent polyubiquitination leading to proteasomal degradation of the $S1P_1$ receptor. This results in unresponsiveness of lymphocytes to S1P.[56]

Potencies of the previously described lipid-based inhibitors all have been determined in assays using unnatural and different ATX substrates (bis-pNPP, pNP-TMP, CPF4 and FS3) as reporter molecules. Therefore it is difficult to compare potencies of distinct inhibitors measured in different assays. In addition, inhibitors in these assays that use unnatural substrates of ATX might have no effect on LPC hydrolysis by ATX due to alternate binding of the substrate. Using assays based on LPC hydrolysis gives a direct answer if ATX inhibitors could inhibit LPA production by ATX. The most potent (IC_{50} = 5.6 nM, LPC) lipid-based inhibitor measured in an LPC hydrolysis assay is S32826 (**9**, Table 2).[39,57,58] This phosphonate inhibitor is a result of screening 13,000 small molecules for their ability to inhibit ATX. Unfortunately, the poor *in vivo* stability and/or bioavailability of the compound did not permit further use in animal models. A last lipid-like inhibitor class is based on a tyrosine building block and an example of this class is inhibitor **10**, which has a micromolar potency (K_i = 1.0 µM, LPC, Table 2).[59-61]

A frequently observed phenomenon for ATX inhibitors is their incapability to fully inhibit ATX. Examples are inhibitors **3**, **4** and **9** depicted in Table 2 that have residual ATX activity (RA) for ATX.

Table 2: Lipid and lipid-based inhibitors of ATX.

Entry	Inhibitor	Substrate	Activity	References [a]
1	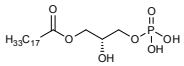 LPA	CPF4	K_i = 0.11 µM	[33]
2	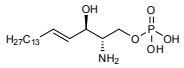 S1P	CPF4	K_i = 0.05 µM	[33]
3	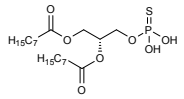 Thiophosphate	Bis-pNPP	IC_{50} = 0.60 µM RA = 27% [b]	[44] [45] [46]
4	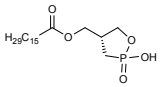 cPA-based	Bis-pNPP	IC_{50} = 0.14 µM RA = 9%	[47] [48]
5	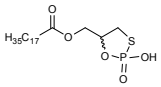 3-*O*-thia-cPA	FS3	PI = 55% @ 10 µM [c]	[49]
6	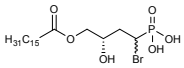 BrP-LPA	FS3	PI = 94% @ 10 µM	[50] [51]
7	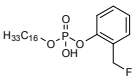 Fluoromethylphenyl	FS3	PI = 95% @ 3 µM	[53]
8	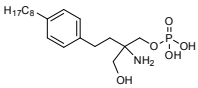 FTY720-P	pNP-TMP	K_i = 0.2 µM	[54] [55]
9	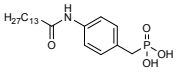 S32826	LPC	IC_{50} = 5.6 nM RA ≈ 10%	[39] [57] [58]
10	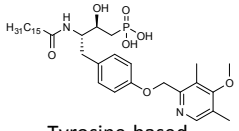 Tyrosine-based	LPC	K_i = 1.0 µM	[59] [60] [61]

[a] First reference corresponds with displayed structure the following references refer to similar inhibitor structures. [b] RA; residual ATX activity. [c] PI; percentage inhibition.

1.7 Small molecule inhibitors of ATX

Since 2008 many small molecule inhibitors have been reported in both academic and patent literature (Table 3). The most potent inhibitor (IC_{50} = 1.7 nM, LPC) reported to date is PF-8380 (**11**).[62,63] Interestingly, this compound reported by employees of Pfizer[62] is based on an inhibitor described in a Merck KGaA patent application.[63] Due to the high potency and favorable pharmacokinetic properties, PF-8380 is a suitable tool compound for *in vivo* evaluation of ATX inhibition.

Another very potent ATX inhibitor is the boronic acid HA155 (**12**, IC_{50} = 5.7 nM, LPC, Table 3), which is described in more detail in Chapter 3 of this thesis.[36,38] This molecule resulted from screening ~40,000 small molecules followed by medicinal chemistry efforts on the resulting screening hit. In the original screening hit a carboxylic acid moiety was replaced by a boronic acid moiety, designed to target the threonine oxygen nucleophile in the ATX active site. HA130,[36,38] a positional boronic acid isomer of HA155 that is described in Chapter 2 and 3, together with PF-8380 are the only two inhibitors to date that have been demonstrated to lower LPA levels *in vivo* (rat or mice).

Recently, other boronic acid-based inhibitors have been reported[64] as a result of a structure-based study resulting in *E*-**28** (**13**, Table 3), a potent inhibitor of ATX (IC_{50} = 5.3 nM, LPC). This study is described in Chapter 4 of this thesis.

A common feature of the three most potent inhibitors reported so far (**11**-**13**, Table 3) is that they share a long linear and flexible structure, which is also reflected in the structure of LPC and LPA. Probably this structural feature helps the inhibitors to accommodate to the lipid binding site since they bind to the ATX active site. Most of the other reported small molecules inhibitors lack this structural feature.

Several Merck KGaA patent applications claim ATX inhibitors (**15**-**18**) with *in vitro* potencies between 0.1 and 10 µM (LPC).[65-71] Structural diversity of these inhibitors is large as can be judged from Table 3.

Screening a phosphodiesterase targeted inhibitor library revealed that Vinpocetin (**19**, Table 3), a PDE type 1 inhibitor (IC_{50} = 8-50 µM), inhibits ATX with an IC_{50} value of 122 µM using LPC as a substrate.[72] In addition, screening a second library consisting of kinase inhibitors known to target the ATP binding site in kinases resulted in the discovery of Damnacanthal (**20**, Table 3), a $p56^{lck}$ tyrosine kinase inhibitor (IC_{50} = 17-620 nM), as ATX inhibitor (IC_{50} = 139 µM, LPC).[72]

Several ATX screening programs used libraries from the National Cancer Institute (NCI). This led for example to the discovery of arsenic acid NSC-48300 (**21**, Table 3) as ATX inhibitor, reported by two independent groups.[38,73,74] It is a competitive inhibitor which could suggest that the arsenic acid moiety in **21** acts as a non-hydrolyzable phosphate mimic. In addition, NSC-9616 (**22**, Table 3) has been identified as ATX inhibitor from screening an NCI library.[75]

The first virtual screen for ATX inhibitors led to the discovery of H2L-7905958 (**23**, Table 3).[76] This inhibitor has a K_i value of 1.9 µM (FS3) for ATX.[77] At the time of this virtual

Table 3: Activities of small molecule inhibitors of ATX.

Entry	Inhibitor	Substrate	Activity	References [a]
11	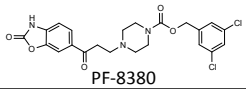 PF-8380	LPC	IC_{50} = 1.7 nM	[62] [63]
12	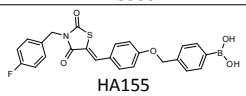 HA155	LPC	IC_{50} = 5.7 nM	[36] [38]
13	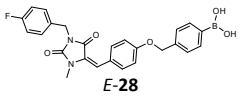 *E*-**28**	LPC	IC_{50} = 5.3 nM	[64]
14	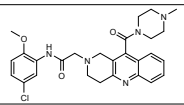	LPC	IC_{50} > 0.1 µM	[65] [66]
15	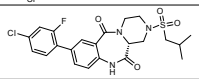	LPC	IC_{50} = 0.1-1 µM	[67] [68]
16	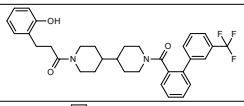	LPC	IC_{50} > 1 µM	[69]
17	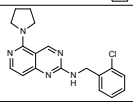	LPC	IC_{50} > 5 µM	[70]
18	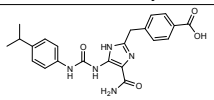	LPC	IC_{50} = 1-10 µM	[71]
19	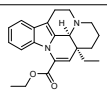 Vinpocetin	LPC	IC_{50} = 122 µM	[72]
20	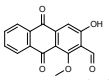 Damnacanthal	LPC	IC_{50} = 139 µM	[72]
21	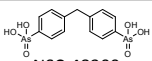 NSC-48300	FS3	K_i = 0.240 µM	[38] [73] [74]
22	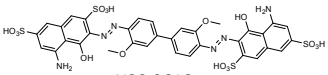 NSC-9616	FS3	K_i = 0.271 µM	[75]
23	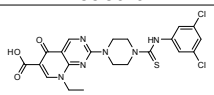 H2L-7905958	FS3	K_i = 1.9 µM	[76] [77]
24	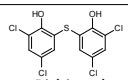 Bithionol	FS3	K_i = 66 µM	[73] [74]

[a] First reference corresponds with displayed structure the following references refer to similar inhibitor structures.

A HA155-ATX structure **B** HA155 targetting the ATX active site

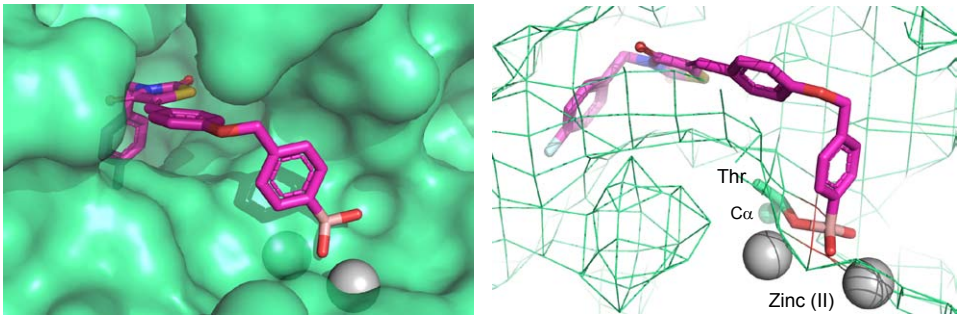

Figure 2: The inhibitor HA155 liganded ATX structure (PD ID 2XRG). (A) Binding of HA155 with ATX. (B) Boronic acid in HA155 targeting the threonine (Thr) oxygen nucleophile and two zinc ions in the ATX active site.

screen the ATX structure was not resolved. Therefore, the authors generated a homology model of ATX based on a *X. axonopodis p*V. *citri* (*Xac*) ENPP structure and used this homology model for virtual screening. Recently, a follow-up study has been reported describing new analogs of **23**.[77]

Another ATX inhibitor is bithionol (**24**, Table 3),[73,74] a known metal ion chelating molecule like L-histidine and EDTA.[78] The latter two inhibit ATX by scavenging metal ions in solution, which are required for ATX activity. However, inhibitor **24** appears to act directly on ATX and not *via* metal chelation since the K_i value of **24** for ATX is two orders of magnitude lower than the used metal ion concentration.

1.8 ATX structure and inhibitor design

In 2011, the crystal structure of ATX has been resolved independently by two groups.[26,79] Next to the unliganded ATX structure, structures of ATX with different species of LPA[26] and the inhibitor HA155 liganded ATX structure[79] have been reported. Binding of HA155 to the ATX active site is predominately driven by hydrophobic interactions and by a boronic acid moiety binding to the threonine oxygen nucleophile in the ATX active site (Figure 2A and B).[79] The latter binding was predicted because the boronic acid moiety in HA155 was designed and introduced to target the threonine oxygen nucleophile in the ATX active site. In addition, the ATX-HA155 structure showed that one of the boronic acid hydroxyl moieties is simultaneously tethered by the two zinc ions in the ATX active site (Figure 2B). Therefore, the boronic acid moiety not only targets the threonine oxygen nucleophile but also the two zinc ions that are essential for catalytic activity of ATX. Another feature of HA155 binding to the ATX active site is that its 4-fluorobenzyl moiety binds to the hydrophobic lipid binding pocket of ATX (Figure 2A), preventing that the alkyl chain of the lipid binds to this pocket.[26,79]

The ATX structure liganded with HA155 triggered an ATX structure-based inhibitor design, which is described in Chapter 4 of this thesis.[64] This study led to *E*-**28** (IC_{50} = 5.3 nM, LPC, Table 3) a hydantoin analog of HA155 (IC_{50} = 5.7 nM, LPC, Table 3). Remarkably, *E*-**28** is an *E*-isomer while HA155 is a *Z*-isomer. To understand how *E*-**28** binds to ATX, molecular docking experiments were performed, which suggested a binding pose for *E*-**28** different from that of the original binding pose of HA155 or from the *Z*-isomer of **28** for ATX. This study predicted that the 4-fluorobenzyl moiety in HA155 and *E*-**28** binds differently to the hydrophobic pocket in ATX. This finding may be used to design new inhibitors that fully exploit the ATX hydrophobic pocket opening further options for inhibitor design.

1.9 Concluding remarks

ATX is an attractive therapeutic target for LPA-related diseases. In the past decade, several ATX inhibitors have been discovered and developed ranging from metal chelators, lipid and lipid-based inhibitors to small molecule inhibitors. Over the last three years many patents on ATX inhibitors have appeared from pharmaceutical industry and academia emphasizing the interest on ATX as drug target. Finally, the recently reported crystal structure of ATX will aid medicinal chemistry efforts to further develop ATX inhibitors into therapeutic agents.

1.10 References

1. Stracke, M. L. et al. Identification, purification, and partial sequence analysis of autotaxin, a novel motility-stimulating protein. *J. Biol. Chem.* **267**, 2524-2529 (1992).
2. Stefan, C. Jansen, S. & Bollen, M. Modulation of purinergic signaling by NPP-type ectophosphodiesterases. *Purinergic. Signal* **2**, 361-370 (2006).
3. Tokumura, A. et al. Identification of human plasma lysophospholipase D, a lysophosphatidic acid-producing enzyme, as autotaxin, a multifunctional phosphodiesterase. *J. Biol. Chem.* **277**, 39436-39442 (2002).
4. Umezu-Goto, M. et al. Autotaxin has lysophospholipase D activity leading to tumor cell growth and motility by lysophosphatidic acid production. *J. Cell Biol.* **158**, 227-233 (2002).
5. Noguchi, K. Herr, D. Mutoh, T. & Chun, J. Lysophosphatidic acid (LPA) and its receptors. *Curr. Opin. Pharmacol.* **9**, 15-23 (2009).
6. Moolenaar, W. H. van Meeteren, L. A. & Giepmans, B. N. The ins and outs of lysophosphatidic acid signaling. *BioEssays* **26**, 870-881 (2004).
7. Sciorra, V. A. & Morris, A. J. Roles for lipid phosphate phosphatases in regulation of cellular signaling. *Biochim. Biophys. Acta* **1582**, 45-51 (2002).
8. Brindley, D. & Pilquil, C. Lipid phosphate phosphatases and signaling. *J. Lipid Res.* **50**, S225-S230 (2009).
9. Tanaka, M. et al. Autotaxin stabilizes blood vessels and is required for embryonic vasculature by producing lysophosphatidic acid. *J. Biol. Chem.* **281**, 25822-25830 (2006).
10. van Meeteren, L. A. et al. Autotaxin, a secreted lysophospholipase D, is essential for blood vessel formation during development. *Mol. Cell Biol.* **26**, 5015-5022 (2006).

11. Mills, G. B. & Moolenaar, W. H. The emerging role of LPA in cancer. *Nat. Rev. Cancer* **3**, 582-591 (2003).
12. Taghavi, P. et al. In vitro genetic screen identifies a cooperative role for LPA signaling and c-Myc in cell transformation. *Oncogene* **27**, 6806-6816 (2008).
13. Nam, S. W. et al. Autotaxin (ATX), a potent tumor motogen, augments invasive and metastatic potential of ras-transformed cells. *Oncogene* **19**, 241-247 (2000).
14. Liu, S. et al. Expression of autotaxin and lysophosphatidic acid receptors increases mammary tumorigenesis, invasion, and metastases. *Cancer Cell* **15**, 539-550 (2009).
15. Boucharaba, A. et al. Platelet-derived lysophosphatidic acid supports the progression of osteolytic bone metastases in breast cancer. *J. Clin. Invest.* **114**, 1714-1725 (2004).
16. Lin, S. et al. The absence of LPA2 attenuates tumor formation in an experimental model of colitis-associated cancer. *Gastroenterology* **136**, 1711-1720 (2009).
17. Kanda, H. et al. Autotaxin, an ectoenzyme that produces lysophosphatidic acid, promotes the entry of lymphocytes into secondary lymphoid organs. *Nat. Immunol.* **9**, 415-423 (2008).
18. Pradere, J. P. et al. LPA1 receptor activation promotes renal interstitial fibrosis. *J. Am. Soc. Nephrol.* **18**, 3110-3118 (2007).
19. Tager, A. et al. The lysophosphatidic acid receptor LPA1 links pulmonary fibrosis to lung injury by mediating fibroblast recruitment and vascular leak. *Nat. Med.* **14**, 45-54 (2008).
20. Pamuklar, Z. et al. Autotaxin/lysopholipase D and lysophosphatidic acid regulate murine hemostasis and thrombosis. *J. Biol. Chem.* **284**, 7385-7394 (2009).
21. Kremer, A. et al. Lysophosphatidic Acid Is a Potential Mediator of Cholestatic Pruritus. *Gastroenterology* **139**, 1008-1018 (2010).
22. Giganti, A. et al. Murine and human autotaxin α, β, and γ isoforms: Gene organization, tissue distribution, and biochemical characterization. *J. Biol. Chem.* **283**, 7776-7789 (2008).
23. Murata, J. et al. cDNA cloning of the human tumor motility-stimulating protein, autotaxin, reveals a homology with phosphodiesterases. *J. Biol. Chem.* **269**, 30479-30484 (1994).
24. Jansen, S. et al. Proteolytic maturation and activation of autotaxin (NPP2), a secreted metastasis-enhancing lysophospholipase D. *J. Cell Sci.* **118**, 3081-3089 (2005).
25. Gijsbers, R. Aoki, J. Arai, H. & Bollen, M. The hydrolysis of lysophospholipids and nucleotides by autotaxin (NPP2) involves a single catalytic site. *FEBS Lett.* **538**, 60-64 (2003).
26. Nishimasu, H. et al. Crystal structure of autotaxin and insight into GPCR activation by lipid mediators. *Nat. Struct. Mol. Biol.* **18**, 205-212 (2011).
27. Clair, T. et al. Autotaxin hydrolyzes sphingosylphosphorylcholine to produce the regulator of migration, sphingosine-1-phosphate. *Cancer Res.* **63**, 5446-5453 (2003).
28. Postma, F. R. Jalink, K. Hengeveld, T. & Moolenaar, W. H. Sphingosine-1-phosphate rapidly induces Rho-dependent neurite retraction: action through a specific cell surface receptor 9. *EMBO J.* **15**, 2388-2392 (1996).
29. Hla, T. Lee, M. Ancellin, N. Paik, J. & Kluk, M. Lysophospholipids-Receptor Revelations. *Science* **294**, 1875-1878 (2001).
30. Ishii, I. Fukushima, N. Ye, X. & Chun, J. Lysophospholipid Receptors: Signaling and Biology. *Annu. Rev. Biochem.* **73**, 321-354 (2004).
31. Spiegel, S. & Milstien, S. Sphingosine-1-phosphate: an enigmatic signalling lipid. *Nat. Rev. Mol. Cell Biol.* **4**, 397-407 (2003).

32. Tokumura, A. Miyake, M. Yoshimoto, O. Shimizu, M. & Fukuzawa, K. Metal-Ion stimulation and inhibition of lysophospholipase D which generates bioactive lysophosphatidic acid in rat plasma. *Lipids* **33**, 1009-1015 (1998).
33. van Meeteren, L. A. et al. Inhibition of autotaxin by lysophosphatidic acid and sphingosine 1-phosphate. *J. Biol. Chem.* **280**, 21155-21161 (2005).
34. Scherer, M. Schmitz, G. & Liebisch, G. High-Throughput Analysis of Sphingosine 1-Phosphate, Sphinganine 1-Phosphate, and Lysophosphatidic Acid in Plasma Samples by Liquid Chromatography-Tandem Mass Spectrometry. *Clin. Chem.* **55**, 1218-1222 (2009).
35. Murph, M. et al. *Methods in Enzymology Lipidomics and* Bioactive Lipids: Specialized Analytical Methods and Lipids in Disease. Brown, H. A. (ed.), pp. 1-25 (2007).
36. Albers, H. M. et al. Boronic acid-based inhibitor of autotaxin reveals rapid turnover of LPA in the circulation. *Proc. Natl. Acad. Sci. USA* **107**, 7257-7262 (2010).
37. Imamura, S. & Horiuti, Y. Enzymatic determination of phospholipase D activity with choline oxidase. *J. Biochem.* **83**, 677-680 (1978).
38. Albers, H. M. et al. Discovery and Optimization of Boronic Acid Based Inhibitors of Autotaxin. *J. Med. Chem.* **53**, 4958-4967 (2010).
39. Ferry, G. et al. S32826, A Nanomolar Inhibitor of Autotaxin: Discovery, Synthesis and Applications as a Pharmacological Tool. *J. Pharmacol. Exp. Ther.* **327**, 809-819 (2008).
40. Takakusa, H. et al. Design and Synthesis of an Enzyme-Cleavable Sensor Molecule for Phosphodiesterase Activity Based on Fluorescence Resonance Energy Transfer. *J. Am. Chem. Soc.* **124**, 1653-1657 (2002).
41. Ferguson, C. et al. Fluorogenic Phospholipid Substrate to Detect Lysophospholipase D/Autotaxin Activity. *Org. Lett.* **8**, 2023-2026 (2006).
42. Cavalli, S. et al. Development of an Activity-Based Probe for Autotaxin. *ChemBioChem* **11**, 2311-2317 (2010).
43. Clair, T. et al. L-histidine inhibits production of lysophosphatidic acid by the tumor-associated cytokine, autotaxin. *Lipids Health Dis.* **4**, 5 (2005).
44. Durgam, G. et al. Synthesis and pharmacological evaluation of second-generation phosphatidic acid derivatives as lysophosphatidic acid receptor ligands. *Bioorg. Med. Chem. Lett.* **16**, 633-640 (2006).
45. Durgam, G. et al. Synthesis, Structure-Activity Relationships, and Biological Evaluation of Fatty Alcohol Phosphates as Lysophosphatidic Acid Receptor Ligands, Activators of PPARγ, and Inhibitors of Autotaxin. *J. Med. Chem.* **48**, 4919-4930 (2005).
46. Gududuru, V. et al. Identification of Darmstoff analogs as selective agonists and antagonists of lysophosphatidic acid receptors. *Bioorg. Med. Chem. Lett.* **16**, 451-456 (2006).
47. Baker, D. et al. Carba Analogs of Cyclic Phosphatidic Acid Are Selective Inhibitors of Autotaxin and Cancer Cell Invasion and Metastasis. *J. Biol. Chem.* **281**, 22786-22793 (2006).
48. Gupte, R. et al. Synthesis and pharmacological evaluation of the stereoisomers of 3-carba cyclic-phosphatidic acid. *Bioorg. Med. Chem. Lett.* **20**, 7525-7528 (2010).
49. Tanaka, R. et al. Efficient synthesis of 3-O-thia-cPA and preliminary analysis of its biological activity toward autotaxin. *Bioorg. Med. Chem. Lett.* **21**, 4180-4182 (2011).
50. Prestwich, G. et al. Antitumor α–Chloro and α–Bromo phosphonate analogs of lysophosphatidic acid. (WO2008157361A1), 65pp. 24-12-2008. University of Utah Research Foundation, USA;

University of Tennessee Research Foundation. Ref Type: Patent

51. Jiang, G. et al. α-substituted phosphonate analogues of lysophosphatidic acid (LPA) selectively inhibit production and action of LPA. *ChemMedChem* **2**, 679-690 (2007).
52. Kumar, S. et al. Activity-based probes for protein tyrosine phosphatases. *Proc. Natl. Acad. Sci. USA* **101**, 7943-7948 (2004).
53. Parrill-Baker, A. Baker, D. & Montedonico, L. Preparation of fluoromethylphenyl phosphodiesters as mechanism-based inactivators of autotaxin. (WO2010040080A1), 38pp. 8-4-2010. USA. Ref Type: Patent
54. van Meeteren, L. Brinkmann, V. Saulnier-Blache, J. Lynch, K. & Moolenaar, W. Anticancer activity of FTY720: Phosphorylated FTY720 inhibits autotaxin, a metastasis-enhancing and angiogenic lysophospholipase D. *Cancer Lett.* **266**, 203-208 (2008).
55. Valentine, W. et al. (S)-FTY720-Vinylphosphonate, an analogue of the immunosuppressive agent FTY720, is a pan-antagonist of sphingosine 1-phosphate GPCR signaling and inhibits autotaxin activity. *Cell. Signalling* **22**, 1543-1553 (2010).
56. Oo, M. et al. Immunosuppressive and Anti-angiogenic Sphingosine 1-Phosphate Receptor-1 Agonists Induce Ubiquitinylation and Proteasomal Degradation of the Receptor. *J. Biol. Chem.* **282**, 9082-9089 (2007).
57. Gupte, R. et al. Benzyl and Naphthalene Methylphosphonic Acid Inhibitors of Autotaxin with Anti-invasive and Anti-metastatic Activity. *ChemMedChem* **6**, 922-935 (2011).
58. Jiang, G. Madan, D. & Prestwich, G. Aromatic phosphonates inhibit the lysophospholipase D activity of autotaxin. *Bioorg. Med. Chem. Lett.* **21**, 5098-5101 (2011).
59. East, J. et al. Synthesis and structure-activity relationships of tyrosine-based inhibitors of autotaxin (ATX). *Bioorg. Med. Chem. Lett.* **20**, 7132-7136 (2010).
60. Cui, P. et al. Synthesis and biological evaluation of phosphonate derivatives as autotaxin (ATX) inhibitors. *Bioorg. Med. Chem. Lett.* **17**, 1634-1640 (2007).
61. Cui, P. McCalmont, W. Tomsig, J. Lynch, K. & Macdonald, T. α- and β-Substituted phosphonate analogs of LPA as autotaxin inhibitors. *Bioorg. Med. Chem.* **16**, 2212-2225 (2008).
62. Gierse, J. et al. A Novel Autotaxin Inhibitor Reduces Lysophosphatidic Acid Levels in Plasma and the Site of Inflammation. *J. Pharmacol. Exp. Ther.* **334**, 310-317 (2010).
63. Schiemann, K. Schultz, M. Blaukat, A. & Kober, I. Preparation of piperidines and piperazines as antitumor agents. (WO2009046841A2), 152pp. 16-4-2009. Merck Patent GmbH, Germany. Ref Type: Patent
64. Albers, H. M. et al. Structure-Based Design of Novel Boronic Acid-Based Inhibitors of Autotaxin. *J. Med. Chem.* **54**, 4619-4626 (2011).
65. Staehle, W. Kober, I. Schiemann, K. Schultz, M. & Wienke, D. Preparation of benzo[b][1,6] naphthyridines as inhibitors of autotaxin for the treatment of tumors. (WO2010060532A1), 142pp. 3-6-2010. Merck Patent GmbH, Germany. Ref Type: Patent
66. Staehle, W. Kober, I. Schiemann, K. Schultz, M. & Wienke, D. Preparation of benzo[b][1,6] naphthyridines as inhibitors of autotaxin for the treatment of tumors. (DE102008059578A1), 66pp. 10-6-2010. Merck Patent GmbH, Germany. Ref Type: Patent
67. Schultz, M. Schiemann, K. & Staehle, W. Heterocyclic compounds as autotaxin inhibitors and their preparation and use in the treatment of tumors. (WO2011006569A1), 218pp. 20-1-2011.

Merck Patent GmbH, Germany. Ref Type: Patent

68. Schultz, M. Schiemann, K. & Staehle, W. Heterocyclic compounds as autotaxin inhibitors and their preparation and use in the treatment of tumors. (DE102009033392A1), 109pp. 20-1-2011. Merck Patent GmbH, Germany. Ref Type: Patent
69. Schiemann, K. Schultz, M. & Staehle, W. Piperidine and piperazine derivatives as autotaxin inhibitors and their preparation and use for the treatment and prophylaxis of cancers and other autotaxin-mediated diseases. (WO2010115491A2), 179pp. 14-10-2010. Merck Patent GmbH, Germany. Ref Type: Patent
70. Schiemann, K. et al. Preparation of 2,5-diamino-substituted pyrido[4,3-d]pyrimidines as autotaxin inhibitors useful in treating cancer. (WO2010063352A1), 177pp. 10-6-2010. Merck Patent GmbH, Germany. Ref Type: Patent
71. Schultz, M. Schiemann, K. Botton, G. Blaukat, A. & Kober, I. Preparation of carbamoylimidazoles as anticancer agents. (WO2009046804A1), 163pp. 16-4-2009. Merck Patent G.m.b.H., Germany. Ref Type: Patent
72. Moulharat, N. Fould, B. Giganti, A. Boutin, J. & Ferry, G. Molecular pharmacology of adipocyte-secreted autotaxin. *Chem.-Biol. Interact.* **172**, 115-124 (2008).
73. Saunders, L. P. et al. Identification of small-molecule inhibitors of autotaxin that inhibit melanoma cell migration and invasion. *Mol. Cancer Ther.* **7**, 3352-3362 (2008).
74. Braddock, D. Small molecule inhibitors of autotaxin, and methods of use for the treatment of cancer. (WO2009151644A2), 82pp. 17-12-2009. Yale University, USA. Ref Type: Patent
75. North, E. J. et al. Pharmacophore Development and Application Toward the Identification of Novel, Small-Molecule Autotaxin Inhibitors. *J. Med. Chem.* **53**, 3095-3105 (2010).
76. Parrill, A. et al. Virtual screening approaches for the identification of non-lipid autotaxin inhibitors. *Bioorg. Med. Chem.* **16**, 1784-1795 (2008).
77. Hoeglund, A. et al. Optimization of a Pipemidic Acid Autotaxin Inhibitor. *J. Med. Chem.* **53**, 1056-1066 (2010).
78. Fogg, A. G. Gray, A. & Burns, D. T. Stability constants of metal complexes of bithionol, fenticlor and hexachlorophene. *Anal. Chim. Acta* **51**, 265-270 (1970).
79. Hausmann, J. et al. Structural basis of substrate discrimination and integrin binding by autotaxin. *Nat. Struct. Mol. Biol.* **18**, 198-204 (2011).